Maíra M. Garcia*, Maryam Vatanchi, Khallil T. Chaim, Maria C. G. Otaduy, Andreas Rennings, Daniel Erni, and Waldemar Zylka

Investigating the influence of dielectric pads in 7T magnetic resonance imaging – simulated and experimental assessment

https://doi.org/10.1515/cdbme-2020-3007

Abstract: Dipole radiofrequency (RF) elements have been successfully used to compose multi-channel RF coils for ultra-high fields (UHF) magnetic resonance imaging (MRI). As magnetic components of RF fields (B_1) can be very inhomogeneous at UHF ($B_0 \geq$7T), dielectric pads with high dielectric constants were proposed to improve the B_1 efficiency and homogeneity [1]. Dielectric pads can be used as a passive B_1 shimmimg technique thanks to inducing a strong secondary magnetic field in their vicinity. The use of such dielectric pads affect not only the B_1 field but also the electric field. This in turn affects the specific absorption rate (SAR) and consequently the temperature distribution inside the patient's body. To study these effects, a 29 cm-long transmission dipole RF coil element terminated by two meander was used for 7T MRI [2]. Using a cylindrical agarose-gel phantom, numerical and experimental results were analyzed with respect to homogeneity and amplitude of the magnetic and electric fields generated by the RF element in various configurations with and without dielectric pads. Calculated and measured B_1 results were cross-checked and found to be in good agreement. When using dielectric pads B_1 homogeneity and magnitude increase in regions where it was previously weak or insufficient. Calculations suggest that SAR distribution will change when using the pads.

Keywords: 7T MRI, dielectric pads, experiment, electromagnetic simulation, dipole RF coil, phantom, B_1, homogeneity, SAR, MRI safety.

***Corresponding author: Maíra M. Garcia,** General and Theoretical Electrical Engineering (ATE), University of Duisburg-Essen, and CENIDE – Center of Nanointegration Duisburg-Essen, D-47048 Duisburg, Germany, and Faculty of Electrical Engineering and Applied Natural Sciences, Westphalian University, Campus Gelsenkirchen, Germany, e-mail: maira.martins-garcia@stud.uni-due.de

Khallil T. Chaim, Faculdade de Medicina FMUSP, Universidade de Sao Paulo, Sao Paulo, SP, Brazil

Maria C. G. Otaduy, LIM44, Hospital das Clinicas HCFMUSP, Faculdade de Medicina, Universidade de Sao Paulo, Sao Paulo, SP, Brazil

Andreas Rennings, Daniel Erni, General and Theoretical Electrical Engineering (ATE), University of Duisburg-Essen, and CENIDE – Center of Nanointegration Duisburg-Essen, D-47048 Duisburg, Germany

Maryam Vatanchi, Waldemar Zylka, Faculty of Electrical Engineering and Applied Natural Sciences, Westphalian University, Campus Gelsenkirchen, Germany

1 Introduction

In MRI both transmission and receiving of signal are done through RF elements (RF coils). At UHF the magnetic component B_1 of RF fields can be very inhomogeneous inside the body, since the wavelength becomes comparable to the dimensions of the human head. For this reason, the task to create specific RF elements for the use at 7T scanner is challenging. RF coil's design includes a rigorous assessment of the electromagnetic (EM) fields generated and evaluation of patient/object's safety during MRI procedures [2, 3]. However, when a specific RF coil is designed, it is impossible to predict all the usages that the MRI operator can handle: when different sized and shaped objects are analyzed using this coil, there is a detuning and impedance mismatch caused by the different load in the coil, which already generates intrinsic B_1 inhomogeneity. This is a very common problem for patients geometry that differs from the standard human model.

One of the methods to correct the B_1 transmitted field is using passive RF shimming, which can be done by placing high permittivity materials, more commonly, between the patient/object and the coil. Previous studies show that using such dielectric padding also alters SAR distributions and magnitudes, presenting increase or decrease on its magnitude depending on the aim of the measurement [1].

Investigations of the influence of positioning dielectric pads are especially important for 7T MRI brain scanning, due to the comparable dimensions between the human head and the RF wavelength, which is not an issue at lower B_0. In this study, a transmission RF element for 7T MRI was used to analyze the incident RF magnetic field distribution and the impact on it, when using dielectric pads. SAR predictions were done to estimate energy absorption inside the object.

2 Materials and methods

2.1 Dipole coil configuration

The dipole element used in this study was described in [2], but 29cm in length, intending its use as an element in a multi-channel coil for 7T MRI [4]. The element consists of a metallic strip line of width of 15mm terminated by two meander and a metal ground plate printed on Rogers RO4003 substrates (ϵ_r=3.55; thickness t_s=0.5mm; length l_s=290mm; width w_s=100mm), which are separated by 19mm of air and connected at each extremity by a copper strip (thickness t_c=0.5mm; width w_c=15mm) and an end-capacitor (C_e=1pF). The meander geometry is unchanged in comparison to [3]. The matching network consists of two shunt capacitors C_p=5.6pF, a series capacitor C_s=3pF and a balun with 180° delay coaxial cable placed at metal ground plate center (Fig. 1).

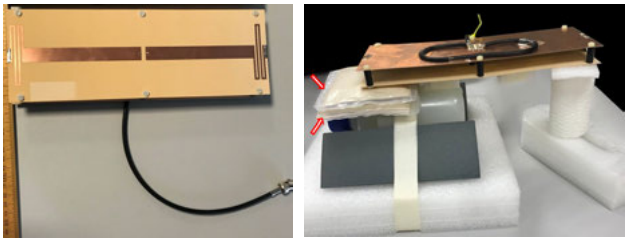

Fig. 1: Left: upper view of the dipole coil element and the coaxial cable. Right: setup to perform one of the experimental measurements: an agarose-gel phantom is placed at one extremity of the dipole coil and the two dielectric pads are indicated by arrows.

2.2 Simulation setup

The design of the dipole coil was done using HFSS (high frequency structure simulator) combined with the Circuit Design tool in the commercially available ANSYS package. Such combination enables the user to perform rapid optimizations and design detailed electronic devices.

The simulation model of the unloaded element in air, including matching network circuit, was continuously improved, in order to obtain a homogeneous magnetic field distribution and a small input reflection coefficient (S11). The final model is very similar to the fabricated dipole coil, counting with a different matching circuit (a series resistor of 41Ω, a series capacitor of 5.36pF, no balun). It is intended to improve the numerical model in order to get as close as possible to the fabricated element, which means, that some losses from the materials, cables and others also need to be counted in the model.

Different simulation scenarios were defined including the loaded coil in conjunction with a virtual phantom and dielectric pads, both with similar characteristics to the phantom and the pads used in the experimental setup (described in 2.3).

Local SAR predictions were done by post-processing the magnitude of electric field $E(\vec{r})$ and the local material properties (σ is specific electrical conductivity, ρ is material mass density, $\vec{r}$ is position vector and V is volume), as in:

$$\mathrm{SAR} = \frac{1}{V}\int_V \frac{\sigma(\vec{r})}{2\rho(\vec{r})}E^2(\vec{r})dV. \quad (1)$$

At 298MHz the material parameters were assumed as: phantom (σ_p=0.92S/m, ϵ_r^p=58.2, ρ_p=1000kg/m^3); dielectric pad (σ_d=0.08S/m, ϵ_r^d=110) [1, 4]. To ensure reliability in the simulated results all the calculations were performed with a very fine mesh, setting the convergence criterion for the adaptive solutions to 0.006.

2.3 Experimental setup

Experiments were performed at the 7T MRI scanner (MAGNETOM 7T, Siemens Healthcare, Germany) installed in the University of São Paulo, São Paulo, Brazil. In order to analyze the influence of dielectric pads, the SIEMENS SA2RAGE pulse sequence was used to obtain the B_1 field maps (TR=2400ms and TE=0.9ms) [5, 6] from a cylindrical agarose-gel based phantom with 13.3cm of height and 7cm of diameter. The dielectric pads had a square shape (11x11x1cm^3) and were filled with a suspension of calcium titanate and deuteruim oxide (D_2O) (mass-mass ratio of 3:1). Four different experimental configurations were analyzed: *Config. 1*: phantom is placed at the center of the dipole element and 2cm under it; *Config. 2*: phantom is positioned at dipole element's lateral (1.7cm outside) and remains 2cm separated from element; *Config. 3*: same setup as in Config. 2 and dielectric pads are inserted in the 2cm gap between phantom and element; *Config. 4*: same setup as in Configuration 3, applying a different power to the dipole element.

3 Results and discussion

3.1 B_1 field distribution

Simulated results. To study the interaction of the phantom with the surrounding magnetic field and to analyze the influence of positioning the dielectric pads (close to the region where the B_1 field is not homogeneous), simulations for the

different configurations were performed and are presented in Fig. 2. A voltage of 77.8V was applied on the element's port.

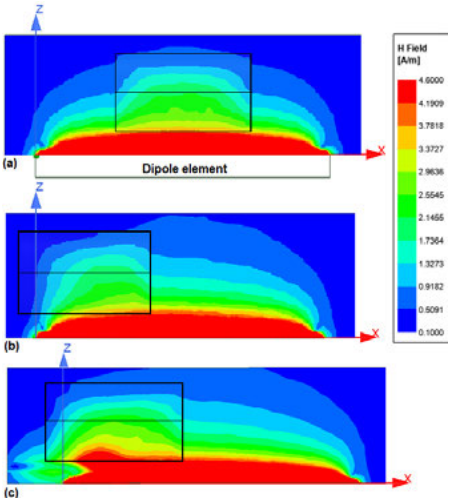

Fig. 2: Simulated results for the magnetic field B_1 strength in a plane xz along the dipole element and positioned at the half width of the element: (a) Config. 1, (b) Config. 2, and (c) Config. 3. The black box represents the phantom, and the central line inside it will be used in Fig. 3.

The B_1 strength distribution in a line positioned in the center of the phantom along x axis (Fig. 2) was compared for the three configurations (Fig. 3). It shows that using dielectric pads, higher B_1 values can be achieved in comparison to Config. 1, presenting similar distribution for a region $x > 30$cm. When compared with phantom lateral positioned (Config. 2) higher B_1 values are achieved in 67.7% of the line.

Experimental results. Magnetic field distributions inside the cylindrical phantom were also measured, as can be seen in Fig. 4. A calibration was done for each configuration to reach the best transmission voltage (Tx) necessary to apply in the dipole element, aiming to get good images. For Config. 1 the voltage 72.2V was applied, the element's excitation for Config. 2 and 3 was 77.8V, and Config. 4 received 155.6V. The same values were used for each corresponding simulation.

It appears that when the phantom is positioned outside the homogeneous region, the magnitude of B_1 is smaller at one side of the phantom and is not high enough to excite equally all the spins (see Fig. 4(b) and Fig. 2(b)). Trying to improve B_1 homogeneity in this region, two dielectric pads were inserted and the same Tx voltage as in Config. 2 was applied, however, this setup didn't generate good images. Due to detuning and mismatching of the dipole element when inserting dielectric pads, the peak of S11 curve has shifted to a lower frequency (as posterior confirmed in a network analyzer) and

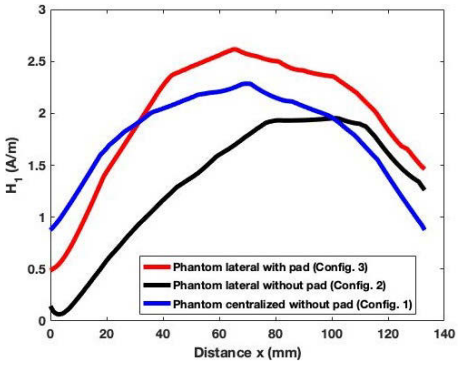

Fig. 3: Magnetic field strength distribution along x line placed in phantom's center (presented in Fig. 2) for Config. 1, 2 and 3.

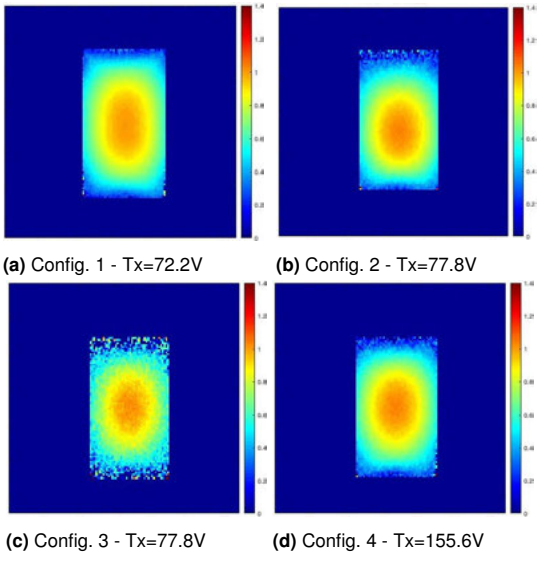

Fig. 4: Magnetic field B_1 distributions measured inside the phantom in the coronal plane taken in the middle of the phantom. Values are normalized to the same color scale.

for this reason, a new calibration was performed and a higher transmission voltage was applied, allowing us to obtain a more homogeneous B_1 field region inside the phantom (Fig. 4(d)).

Simulated versus measured results. Comparisons between calculated and experimental transmitted B_1 fields were carried out for two lines in the central coronal plane: along x and y axis, having as common point the phantom's center (Fig. 5). The comparison of the results shows that the B_1 distribution along x and y, as for z axis (not presented here), are similar in its extension, but differs slightly in amplitude. To achieve the best agreement, the value of end-capacitors in the model was altered to C_e=0.3pF, which could represent not explicitly modeled losses. Using this capacitor value, the simulated coefficient was S11=-48dB while S11=-20dB were measured.

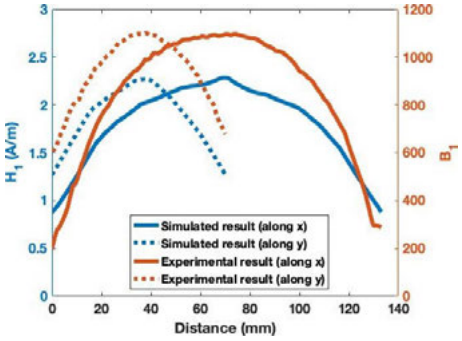

(a) Config. 1.

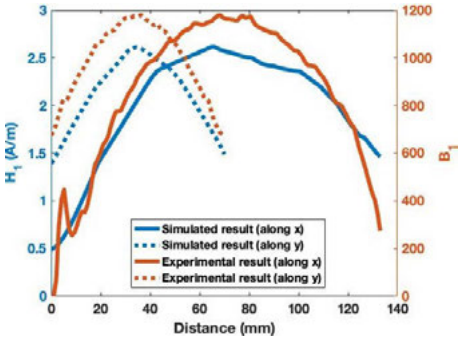

(b) Config. 4.

Fig. 5: B_1 curves along x and y lines in the central coronal plane for simulated and experimental results (where B_1 values represent the percentage times 10 of the attempted flip angle [5]), for setups with (a) and without (b) dielectric pads.

3.2 SAR predictions

As seen in Fig. 2 and 4, dielectric pads positioned near to the phantom can improve B_1 homogeneity inside a region of interest. However, it is also important to analyze how the configuration with pads (Config. 3) will influence the object's energy absorption using our hardware setup, i.e. one dipole coil, phantom and dielectric pads. Simulations in Fig. 6 show different SAR distribution inside the phantom for Config. 3 in comparision to Config. 2, especially in the region that had higher B_1 improvement, presenting no hot-spots and only small changes in SAR. In accordance to [1], SAR variation when using dielectric pads depends on the aim of the measurement and is sequence dependent. Since the aim of this work was to homogenize B_1 inside the whole phantom, an increase in SAR due to the extra loss introduced by the usage of pads was expected.

4 Conclusions

Numerical and experimental investigations show that using dielectric pads can improve the B_1 homogeneity distribution inside an object and can also address higher B_1 magnitude for regions where it was previously not high enough. Additionally, simulations inform that local SAR distribution will change when using pads. The cross-check of results indicates that simulation model and measurement agree very well. However, improvement in the validation process are intended, notably with regard to real losses of the experimental setup, detuning and impedance mismatch when using pads, and calculation of temperature, which can be validated by dedicated MRI sequences.

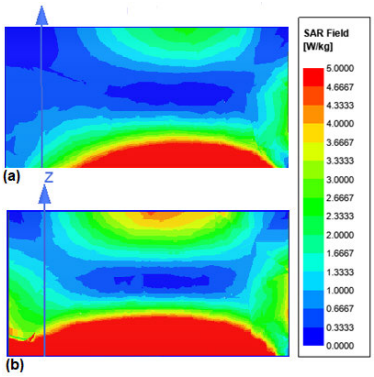

Fig. 6: Local SAR distribution in phantom's central xz plane (x axis is pointing to the right) for (a) Config. 2, and (b) Config. 3.

Author Statement

Research funding: MMG was supported by the Coordination for the Improvement of Higher Education Personnel (CAPES): Full PhD Program Abroad (Programa de Doutorado Pleno no Exterior), process n. 88881.173609/2018-01. Conflict of interest: Authors state no conflict of interest.

References

[1] Teeuwisse W M, Brink W M, Webb A G. Quantitative assessment of the effects of high-permittivity pads in 7 T MRI of the brain. Mag. Reson. Med. 2012;67:1285-1293.

[2] Chen Z, Solbach K, Erni D, Rennings A. Dipole RF element for 7 Tesla magnetic resonance imaging with minimized SAR. 7th EUCAP 2013;1775-1778.

[3] Orzada S, Bahr A, Bolz T. A novel 7T microstrip element using meanders to enhance decoupling. 16th Proc. Intl. Soc. Mag. Reson. Med. 2008; 2979.

[4] Chen Z, Solbach K, Erni D, Rennings A. Electromagnetic field analysis of a dipole coil element with surface impedance characterized shielding plate for 7-Tesla MRI. IEEE Trans. Microw. Theory Techn. 2016;64(3):972-981.

[5] Siemens Application Guide: "SA2RAGE - Work-in-progress package for fast B_1 mapping", Siemens AG, v. 1.0, 2011.

[6] Marques JP, Kober T, Krueger G, Van der Zwaag W, Van de Moortele PF, Gruetter R. MP2RAGE, a self bias-field corrected sequence for improved segmentation and T_1-mapping at high field. NeuroImage 2010;49:1271-1281.